Preparation and Properties of Styrene–Butadiene Rubber Based Nanocomposites: The Influence of the Structural and Processing Parameters

Susmita Sadhu, Anil K. Bhowmick

Rubber Technology Centre, Indian Institute of Technology, Kharagpur 721302, India

Received 10 March 2003; accepted 18 September 2003

ABSTRACT: Rubber-based nanocomposites were prepared with octadecyl amine modified sodium montmorillonite clay and styrene–butadiene rubber with different styrene contents (15, 23, and 40%). The solvent used to prepare the nanocomposites, the cure conditions, and the cure system were also varied to determine their effect on the properties of the nanocomposites. All the composites were characterized with X-ray diffraction (XRD), Fourier transform infrared (FTIR) spectroscopy, and transmission electron microscopy (TEM). The XRD studies revealed exfoliation for the modified clay–rubber composites. The TEM photomicrographs showed a uniform distribution of the modified clay in the rubber matrix. The thickness of the particles in the exfoliated composites was around 10–15 nm. Although the FTIR study of the unmodified and modified clays showed extra peaks due to the intercalation of the amine chains into the gallery, the spectra for the rubber–clay nanocomposites were almost the same because of the presence of a very small amount of clay in the rubber matrix. All the modified clay–rubber nanocomposites displayed improved mechanical strength. The styrene content of the rubber had a pronounced effect on the properties of the nanocomposites. With increasing styrene content, the improvement in the properties was greater. Dicumyl peroxide and sulfur cure systems displayed similar strength, but higher elongation and slightly lower modulus values were obtained with the sulfur cure system. The curing of the samples at four different durations at 160°C showed that the cure time affected the properties. © 2004 Wiley Periodicals, Inc. J Appl Polym Sci 92: 698–709, 2004

Key words: elastomers; clay; nanocomposites; rubber

INTRODUCTION

Polymer–clay interactions were actively studied during the early 1970s. However, the Toyata group has only recently discovered that it is possible to prepare a polymer–clay nanocomposite based on nylon and an organophilic clay,[1] which shows a dramatic improvement in the mechanical, thermal, and barrier properties at very low clay contents in comparison with the unmodified polymer. The term *nanocomposite* describes a two-phase material in which one of the phases is dispersed in the second one on a nanometer level (10^{-9} m).

On the basis of the structure of the clay (Fig. 1) and the nature of the clay–polymer composites, three types of composites (Fig. 2) have been described: conventional composites, in which the clay acts as a conventional filler [Fig. 2(a)]; intercalated nanocomposites, which consist of regular insertions of the polymer between the clay layers [Fig. 2(b)]; and delaminated nanocomposites, in which thin layers are dispersed in a polymer matrix [Fig. 2(c)]. The last structure is the most interesting because of the greater clay–polymer interaction, which makes the entire surface of the clay available to a polymer. This causes maximum changes in the mechanical and physical properties.

The Toyata discovery has encouraged many researchers to develop new polymer-based nanocomposites. Plastics such as nylon,[1–5] polypropylene,[6–8] polyethylene, poly(ethylene oxide), and polystyrene[9] have been used as base polymers for nanocomposites. Very sharp improvements in the mechanical and dynamic mechanical properties have been reported. Rubber-like nanocomposites with natural rubber[10] and ethylene vinyl acetate[11,12] have also been developed. Recently, Ray and Bhowmick[13] prepared an Engage-based nanocomposite by an *in situ* polymerization method. The mechanical properties of styrene–butadiene rubber (SBR)[14–16] based nanocomposites have also been reported by Mousa and Karger-Kocsis[14] and Sadhu and Bhowmick.[16]

However, there has been no study on the effects of the styrene content of SBR, the solvent used for preparation, the cure time, the cure system, and the aging on the morphology and mechanical properties of these nanocomposites. This article reports our observations on the aforementioned studies.

Correspondence to: A. K. Bhowmick (anilkb@rtc.iitkgp.ernet.in).

Journal of Applied Polymer Science, Vol. 92, 698–709 (2004)

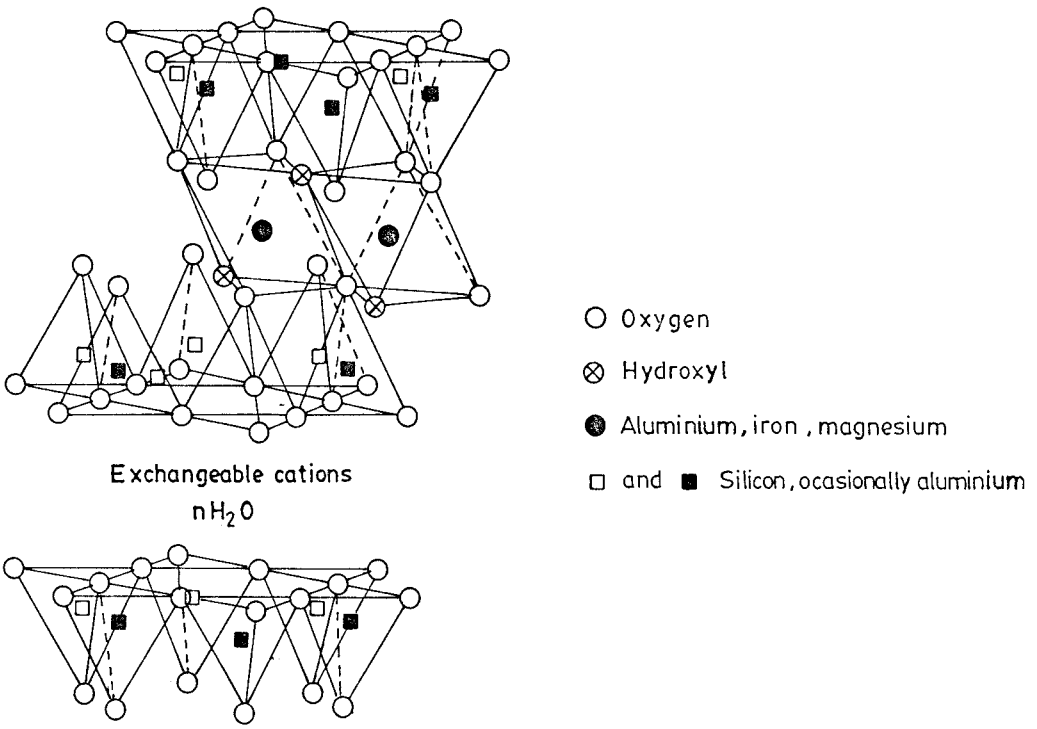

Figure 1 Structure of the tetrahedral–octahedral–tetrahedral montmorillonite clay.

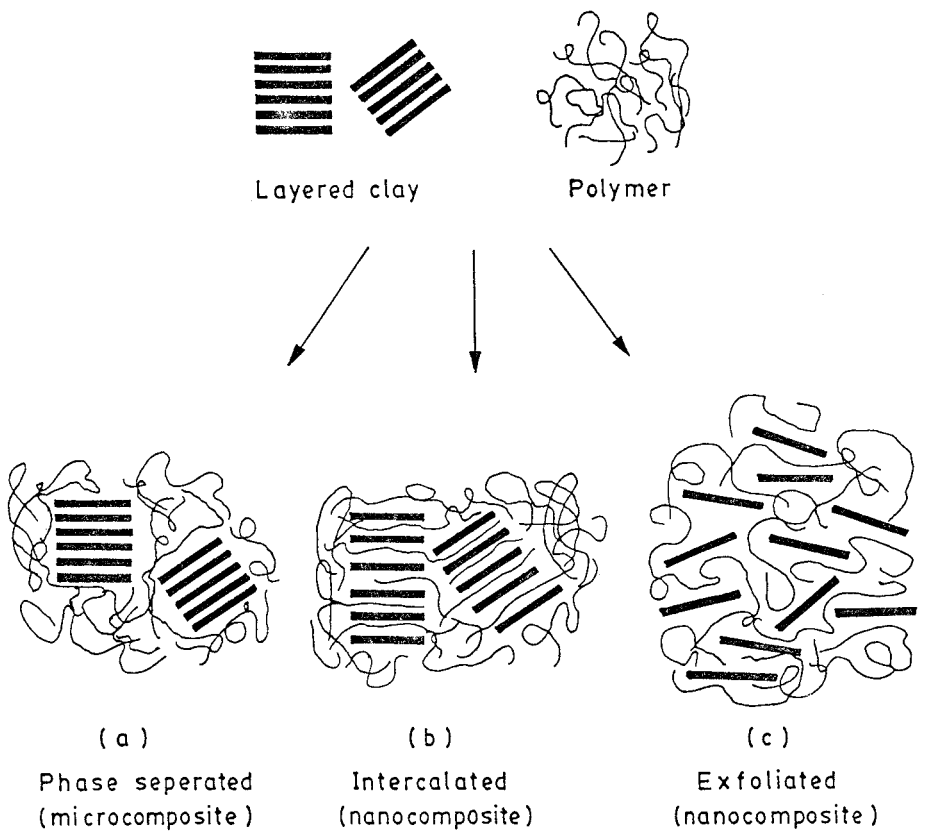

Figure 2 Different types of nanocomposites: (a) conventional, (b) intercalated, and (c) exfoliated.

TABLE I
Materials and Abbreviations

Material	Abbreviation
Unmodified sodium montmorillonite	N
Modified montmorillonite	OC
Styrene–butadiene rubber with 23% styrene content	23SBR
Styrene–butadiene rubber with 40% styrene content	40SBR
Styrene–butadiene rubber with 15% styrene content	15SBR

EXPERIMENTAL

Materials

SBR (Synaprene 1502), with a styrene content 23.5% [Mooney viscosity (M_v) = 52], was supplied by Synthetics and Chemicals, Ltd. (Bareilley, India). Other SBRs, with 15 (M_v = 131) and 40% (M_v = 75) styrene contents, were supplied by Apcotex Lattices, Ltd. (Mumbai, India). Toluene (analytical-grade) was procured from Merck, Ltd. (Mumbai, India); chloroform and carbon tetrachloride were supplied by Ranbaxy, Ltd. (S.A.S. Nagar, India) and Glaxo, Ltd. (Mumbai, India), respectively. Na^+-montmorillonite was generously supplied by Southern Clay Products (Gonzales, TX). Its cation-exchange capacity was 90 mequiv/mol. The amine used was stearyl amine from Sigma Chemical Co. (St. Louis, MO). Dicumyl peroxide (DCP), produced by Hercules, Inc. (Wilmington, DE), was used as the crosslinking agent for SBR. Bengal Chemicals & Pharmaceuticals (Calcutta, India) supplied ethyl alcohol (rubber-grade). Sulfur, tertiary butyl benzthiazole sulfenamide (TBBS), stearic acid, and ZnO for vulcanization studies were procured from the local market.

Preparation of the modified clay

The clay (5 g) was mixed with 400 cc of water, and the mixture was stirred thoroughly at 80°C for half an hour. Then, 2 g of stearyl amine (depending on the equivalent weight) was mixed with concentrated HCl (5 cc), and the mixture was stirred for a few minutes with the addition of 200 cc of water. This solution was then mixed with the clay dispersion with constant slow stirring at 80°C to obtain the modified clay. This modified clay was then filtered and washed thoroughly with hot water until it was confirmed by $AgNO_3$ testing to be free of chloride ions. The modified clay was dried in a vacuum oven at room temperature (30°C).

Preparation of the clay–rubber nanocomposite

The rubber was dissolved in toluene in all cases unless otherwise mentioned. Chloroform and carbon tetrachloride were used to study the variations of the solvent. The clay was dispersed in ethyl alcohol with a magnetic stirrer for half an hour. Then, the rubber solution was mixed with the clay dispersion, and the mixture was stirred for 2 h. The curing agent DCP (1 phr) was added during this stirring. After a homogeneous mixture was obtained, the composite was dried in an oven at 50°C. However, for the sulfur vulcanization system, the cure package (5 phr ZnO, 1.5 phr stearic acid, 1 phr TBBS, 2 phr S) was mixed in an open roll mill after the drying of the rubber–clay mixtures without DCP because not all the ingredients were soluble in the aforementioned organic solvents. All the composites were passed through the mill before being molded at 160°C for 15 min for DCP curing and for 22.5 min for sulfur curing (the cure time at 160°C was obtained with an R100s oscillating disc rheometer (Monsanto, Akron, OH)). A list of the abbreviations used and the designations of the composites prepared are given in Tables I and II, respectively.

X-ray diffraction (XRD) studies

For the characterization of the clays and rubber composites, XRD studies were performed with a Rigaku Miniflex CN2005 X-ray diffractometer from 3 to 10°

TABLE II
Designations of the Nanocomposites

Composition	Designation
15SBR + DCP (1 phr)	15SBR
15SBR + DCP (1 phr) + N (4 phr)	15SBRN4
15SBR + DCP (1 phr) + OC (4 phr)	15SBROC4
23SBR + DCP (1 phr)	23SBR
23SBR + DCP (1 phr) + N (4 phr)	23SBRN4
23SBR + DCP (1 phr) + OC (4 phr)	23SBROC4
40SBR + DCP (1 phr)	40SBR
40SBR + DCP (1 phr) + N (4 phr)	40SBRN4
40SBR + DCP (1 phr) + OC (4 phr)	40SBROC4
23SBR + DCP (0.5 phr)	23SBR(0.5)
23SBR + DCP (0.5 phr) + N (4 phr)	23SBRN4(0.5)
23SBR + DCP (0.5 phr) + OC (4 phr)	23SBROC4(0.5)
23SBR + S-SYSTEM	23SBR(S)
23SBR + S-SYSTEM + OC (4 phr)	23SBROC4(S)
23SBR + S-SYSTEM + N (4 phr)	23SBRN4(S)
23SBR + DCP (1 phr; *X* = 10, 15, 30, and 60) cured for *X* min	23SBR-*X*
23SBR + DCP (1 phr) + N (4 phr; *X* = 10, 15, 30, and 60) cured for *X* min	23SBRN4-*X*
23SBR + DCP (1 phr) + OC (4 phr; *X* = 10, 15, 30, and 60) cured for *X* min	23SBROC4-*X*
23SBR + DCP (1 phr) + OC (4 phr; toluene as solvent)	23SBROC4*
23SBR + DCP (1 phr) + OC (4 phr; carbon tetrachloride as solvent)	Ca-23SBROC4
23SBR + DCP (1 phr) + OC (4 phr; chloroform as solvent)	Ch-23SBROC4

In all of the cases except where it is mentioned, toluene was used as the solvent. The cure time of all of the samples unless mentioned was 15 min at 160°C.

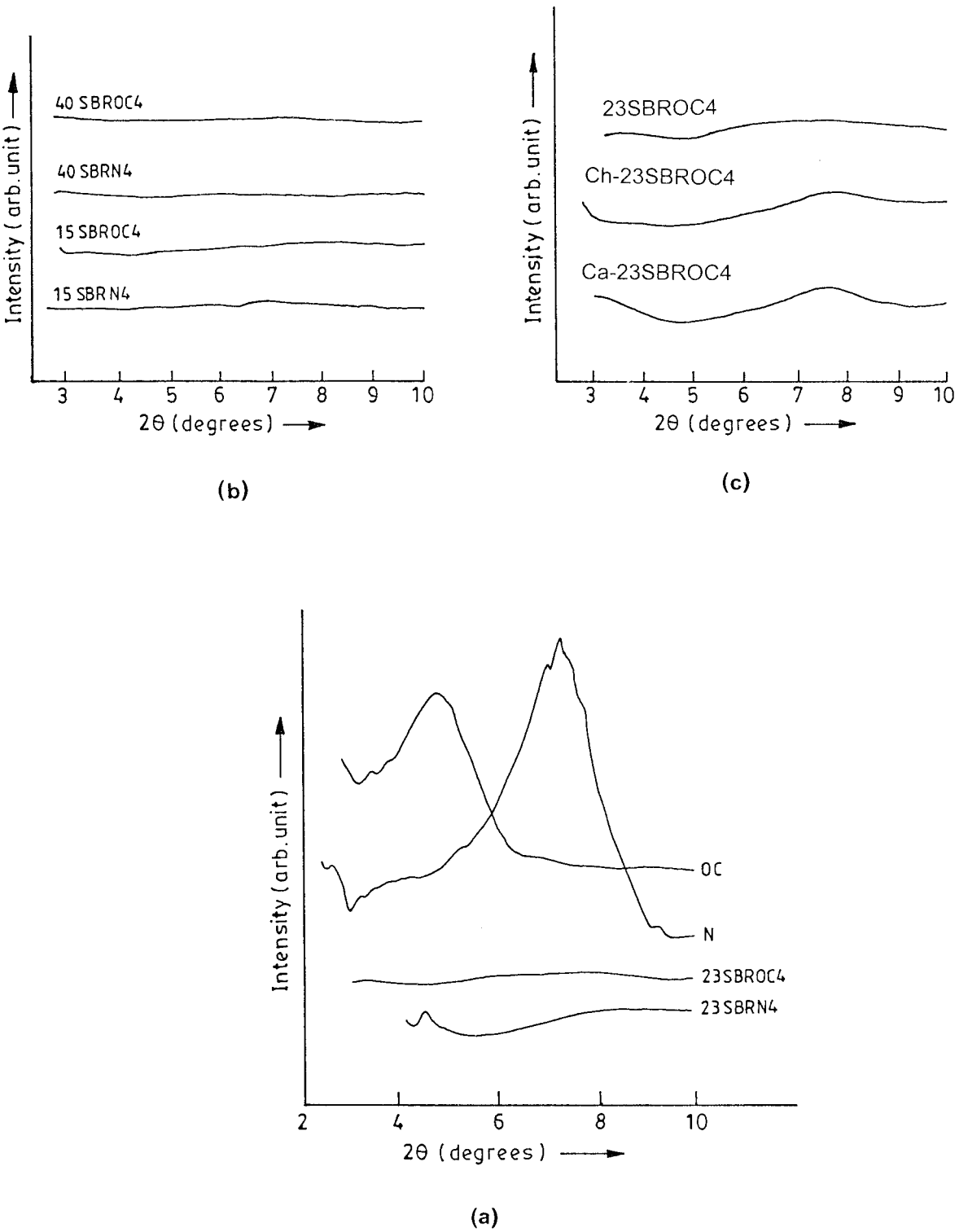

Figure 3 XRD spectra of clays and SBR–clay composites: N, OC, 23SBRN4, 23SBROC4, 15SBRN4, 15SBROC4, 40SBRN4, 40SBROC4, Ca-23SBROC4, 23SBROC4, and Ch-23SBROC4.

(2θ). Then, the d-spacing of the clay particles was calculated with Bragg's equation:

$$n\lambda = 2d \sin \theta \quad (1)$$

where λ is the wavelength of the X-ray (for the copper target used here, λ was 1.54 Å), d is the interspace distance, and θ is the angle of incident radiation.

Fourier transform infrared (FTIR) spectroscopy

For the determination of the interactions between the filler and amine and between the filler and rubber, a

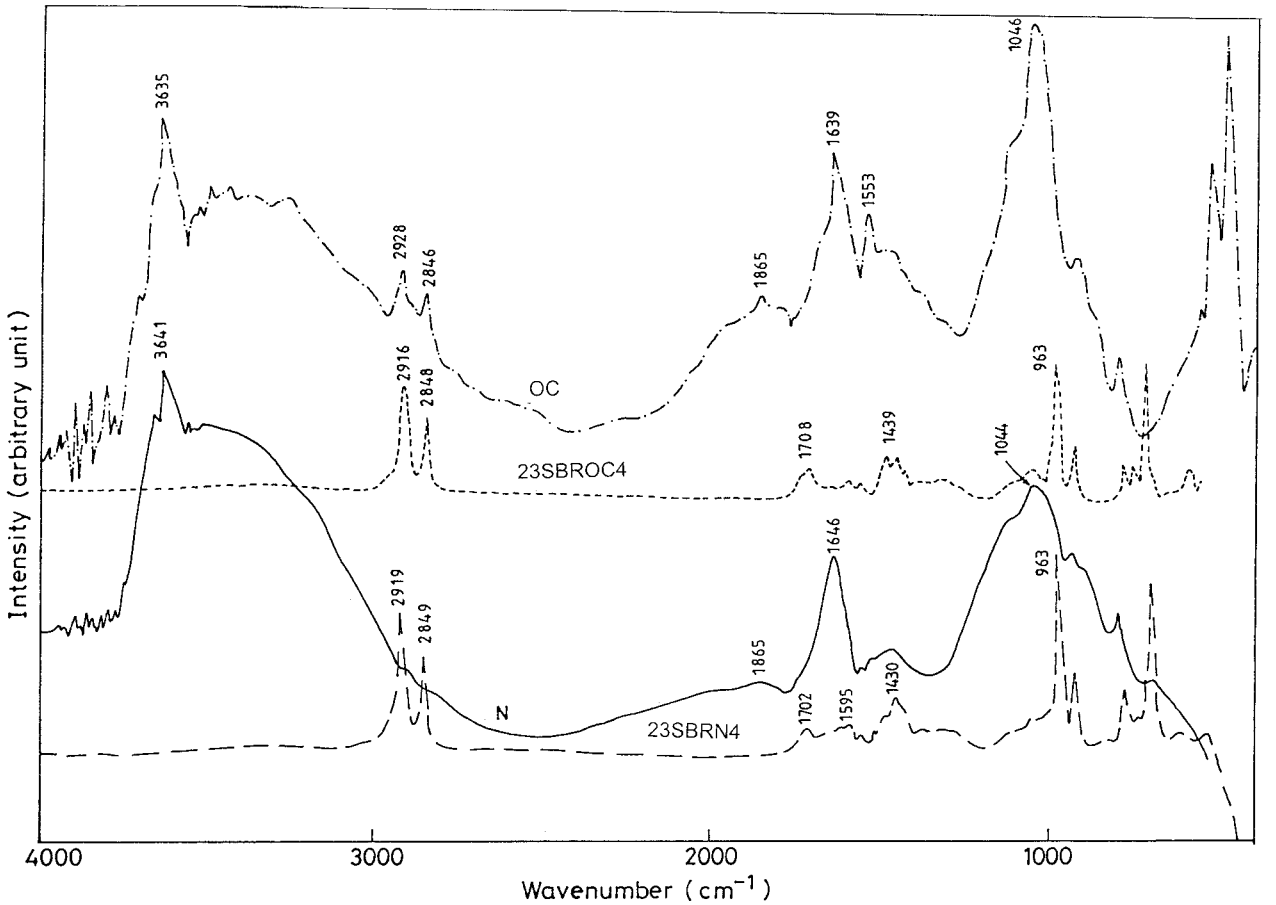

Figure 4 FTIR spectra of N, OC, 23SBRN4, and 23SBROC4.

Nicolet Nexus FTIR instrument was used with a resolution of 4 cm^{-1}. Diffuse reflectance infrared Fourier transform and attenuated total reflection were used from 4000 to 400 cm^{-1} and at 600 cm^{-1} for the powder clay samples and rubber composites (1 mm thick), respectively.

Transmission electron microscopy (TEM)

A Hitachi H-600 electron microscope operating at an accelerating voltage of 100 kV was used. The samples were prepared according to an ASTM procedure.[17]

Mechanical properties

The tensile specimens were punched out from molded sheets with an ASTM Die C. The tests were carried out according to ASTM D 412-98 in a Zwick 1445 universal testing machine at a crosshead speed of 500 mm/min at 25°C. The averages of three tests and their standard deviations are reported here.

RESULTS AND DISCUSSION

Modification and characterization of the nanoclays

The clay was modified with octadecyl amine and characterized by XRD (Fig. 3) and FTIR (Fig. 4). Figure 3(a) shows that there is a peak shift from 7.5 to 4.9° upon the modification of the clay. The XRD results (Table III) show an increase in the gallery gap from 11.6 to 18.2 Å corresponding to this shift. Earlier workers observed a peak in the range of 4–6° for modified nanoclays.[6,16] The FTIR study also shows the presence of extra peaks for the modified clay around 2928 and 2846 cm^{-1} for CH_2 and also around 1865 cm^{-1} for the presence of the $^{+}$NH group, in addition to the peaks present in the unmodified clay around 3635 cm^{-1} for OH groups, around 1640 cm^{-1} due to OH bending, and around 1046 cm^{-1} for Si—O—Si linkages (Fig. 4). These results indicate the intercalation of the aliphatic

TABLE III
XRD Results for the Clay and Nanocomposites

Sample	2Θ (°)	*d*-spacing(Å)
N	7.5	11.6
OC	4.9	18.2
15SBRN4	No peak	Exfoliated
15SBROC4	No peak	Exfoliated
23SBRN4	4.4	20.2
23SBROC4	No peak	Exfoliated
40SBRN4	No peak	Exfoliated
40SBROC4	No peak	Exfoliated

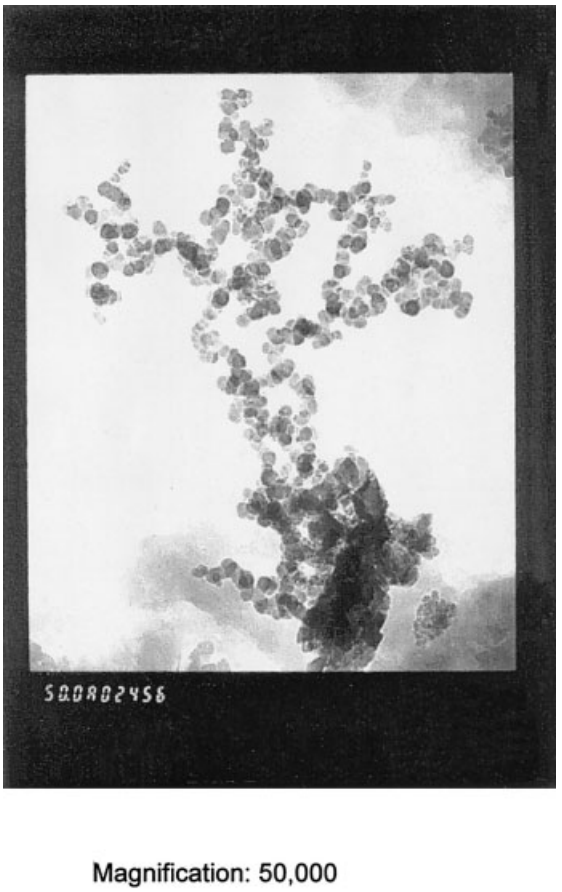

Figure 5 TEM photomicrograph of OC.

amine within the gallery. The particle diameters were measured to be 40–50 nm for the modified clays, as shown in Figure 5. According to a comparison with the TEM results reported in our earlier article,[16] this has a higher structure.

Effect of the organically modified clay on the mechanical properties and morphology of SBR

23SBR was used as the base polymer to study the effects of the nanofillers on the mechanical properties of the polymer (Table IV). The strength of the gum vulcanizate of 23SBR cured with DCP was 1.20 MPa. Upon the addition of unmodified sodium montmorillonite (N), the strength increased to 1.80 MPa. There was a further increase in the strength (38%) up to 2.50 MPa upon the incorporation of the nanoclay at the same loading. The elongation at break and the modulus at 50% elongation changed from 111 to 167% and from 0.66 to 0.77 MPa, respectively, when 4% modified clay was added to SBR. This can be explained with the help of XRD results (Fig. 3 and Table III). There was a small peak around 4.4° in 23SBRN4. However, that peak was absent in 23SBROC4. This proved that the polymer was intercalated into the gallery gap of the clay in 23SBRN4 and increased the distance between the two layers, but the clay was not fully exfoliated. A small fraction of the clay could still have a layered structure. However, 23SBROC4 showed full exfoliation; therefore, there was no peak. The TEM results corroborated the same findings. The particle size was 40–50 nm for 23SBRN4 and 10–15 nm for 23SBROC4 [Fig. 6(a,b)]. The photomicrographs also show a dispersion problem in 23SBRN4, but the clay was well dispersed in 23SBROC4. The FTIR spectra do not give any additional information for the clay nanocomposites (Fig. 4). Because the clay was added in very low amounts, peaks due to the presence of the clay were very weak or undetectable.

On the basis of these results, we concluded that the mechanical properties were improved for 23SBRN4 because of the intercalation within the gallery gap, although the clay was not fully exfoliated there. However, the sharp improvement in the properties of 23SBROC4, compared with those of the gum vulcanizate and 23SBRN4, was due to the total exfoliation and better interaction between the polymer chains and the clay surface modifier.

Effects of the styrene content in SBR on the X-ray and mechanical properties of the nanocomposites

XRD spectra of various clay–rubber composites are given in Figure 3(a–c). There is a small peak around 4.4° for 23SBRN4, but there is no peak for 15SBRN4 or 40SBRN4. The modified clay–rubber composites of all three grades also displayed complete exfoliation. There is no peak for any of the SBROC4s. The XRD results can be explained in the following way. The unmodified clay (N) had a smaller gallery gap (11.6 Å) than the modified clay [i.e., modified montmorillonite (OC); 18.2 Å]. Therefore, a higher degree of intercalation was necessary to cause the exfoliation of OC in comparison with N. In this respect, 15SBR was the least bulky and 40SBR with a higher styrene content

TABLE IV
Influence of the Styrene Content on the Mechanical Properties of the Nanocomposites

Sample	Tensile strength (MPa)	Elongation at break (%)	Modulus at 50% elongation (MPa)	Work to break (J/m^2)
15SBR	1.55	34	—	116
15SBRN4	1.46	59	1.23	185
15SBROC4	1.65	61	1.37	227
23SBR	1.20	111	0.66	284
23SBRN4	1.80	152	0.58	606
23SBROC4	2.50	167	0.77	911
40SBR	5.20	155	2.18	2070
40SBRN4	5.33	256	2.53	2339
40SBROC4	8.20	190	2.74	3988

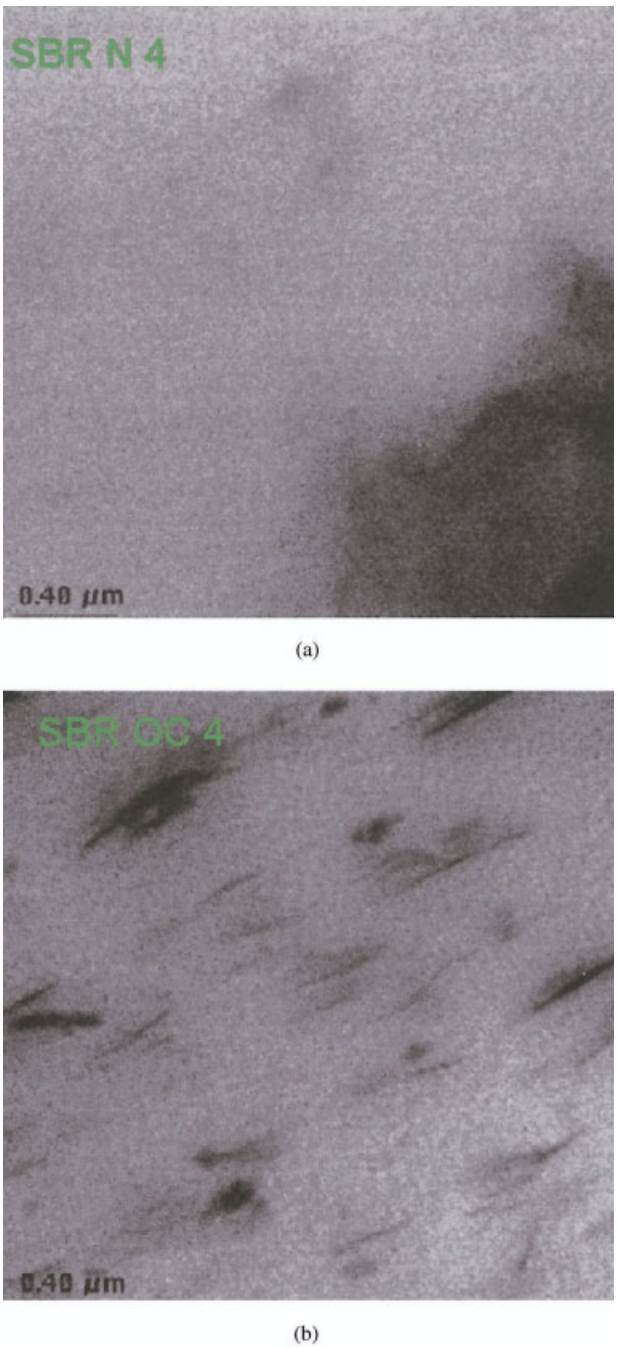

Figure 6 TEM photomicrographs of (a) 23SBRN4 and (b) 23SBROC4.

was the most bulky in the group of three. The bulkier the polymer chain was, the more effective it was in the exfoliation of the clay. However, 15SBR chains had higher segmental mobility than the 40SBR chains. When 15SBR was added to the unmodified clay, the chains, because of less bulkiness, could intercalate into the gap very easily and cause exfoliation. However, SBR with a 40% styrene content could cause exfoliation once it entered the gallery gap. In the case of 23SBR samples, the interplay of both factors took place. Therefore, the rubber intercalated to a large extent into the gallery gap of the clay but could not exfoliate it fully. Hence, a small peak was observed for 23SBRN4, showing the partial exfoliation of the clay, whereas 40SBRN4 revealed no peak.

The TEM study also supports these observations. The photomicrographs show that there was a dispersion problem in 23SBRN4, but the modified clay was uniformly dispersed in 23SBROC4 (Fig. 6).

The effects of the styrene content in SBR on the mechanical properties of the nanocomposites were studied. For this purpose, three different grades of SBR with styrene contents of 15, 23, and 40% were chosen. The stress–strain curves are given in Figures 7–9. The data for 23SBR were taken from our earlier article.[16] The clays, both unmodified and modified, influenced the stress–strain curve. This was significant because the styrene content was higher. An increase in the styrene content increased the ultimate stress. The results are summarized in Table IV. In the case of 15SBR, the tensile strength of the gum vulcanizate was 1.55 MPa; this became 1.46 and 1.65 MPa for 15SBRN4 and 15SBROC4, respectively. The values were 1.20, 1.80, and 2.50 MPa when the styrene content was 23%. 40SBR had a gum vulcanizate strength of 5.20 MPa, whereas the tensile strength of the unmodified clay–rubber composite was 5.33 MPa, and that of the modified clay–rubber composite was 8.20 MPa at the same loading of the filler (Fig. 9 and Table IV). The values of the elongation at break showed a marked increase from that of the gum vulcanizate upon the modification of the clay. The increases were up to 61, 167, and 190% for 15SBR, 23SBR, and 40SBR, respectively. The modulus showed the same trend. In every case, it changed significantly from that of the gum rubber. The mechanical properties of SBROC4s are plotted against the styrene content (Fig. 10). A dramatic improvement took place at a 40% styrene concentration. With increasing styrene content, the glass-transition temperature increased, and so the strength and modulus were greater.

These results completely agree with the structural changes. These were attributed to the exfoliation of the clay in the rubber matrix and to the favorable interaction between the modified filler and rubber. As the unmodified clay was added, the rubber chains intercalated into the gallery gap of the clay and exfoliated it. However, the unmodified clay was an inorganic substance incompatible with the organic rubber matrix. Therefore, because of intercalation and subsequent exfoliation, there were slight increases in the strength, elongation at break, and modulus. The increase in the modulus could also be attributed to the addition of inorganic particles to the rubber matrix and to the increasing number of particles due to the exfoliation of the clay. However, as OC was added to the polymer, the change in the strength was significant: a 53% change in the tensile strength, a 23%

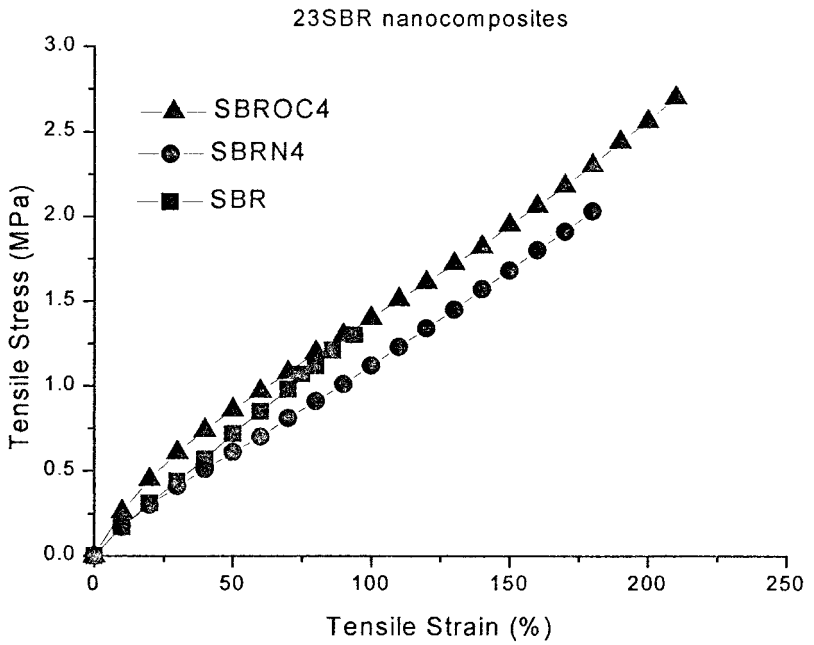

Figure 7 Stress–strain plots of 23SBR with and without clay.

change in the elongation at break, and a 25% change in the modulus at 50% elongation for 40SBROC4 in comparison with those of the gum vulcanizate. The polymer had a favorable nonpolar–nonpolar interaction with the clay, which helped in the total exfoliation of the clay and in the increasing physical bonding with the rubber. Therefore, these two factors were responsible for the improvement in the tensile strength, elongation at break, and modulus at 50% elongation. The changes in the mechanical properties in the other two SBR grades were similar and could be explained in a similar way.

Effect of the solvent on the properties of the nanocomposites

The effect of the solvent used during the preparation of the nanocomposite was also studied. For this purpose, three solvents (toluene, chloroform, and carbon

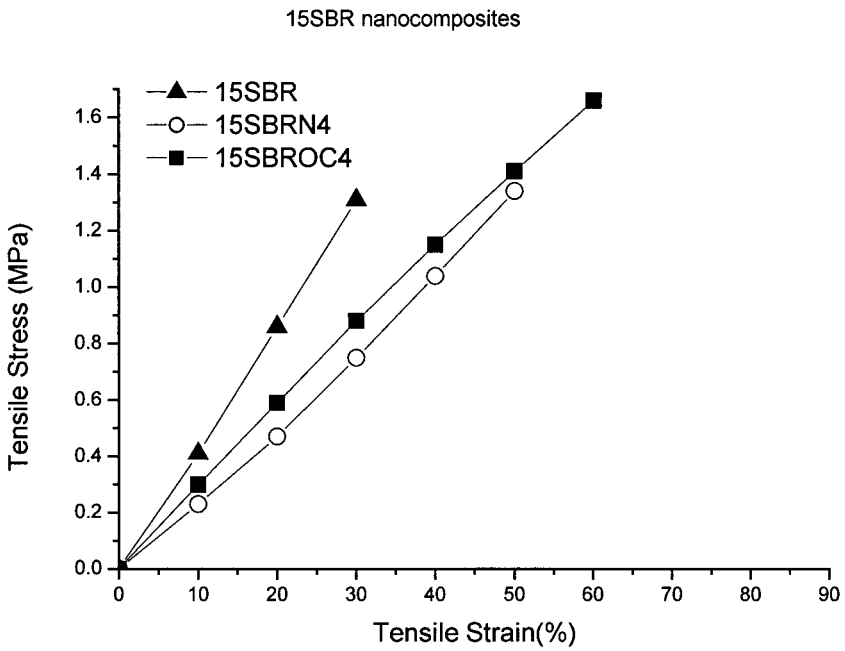

Figure 8 Stress–strain plots of 15SBR with and without clay.

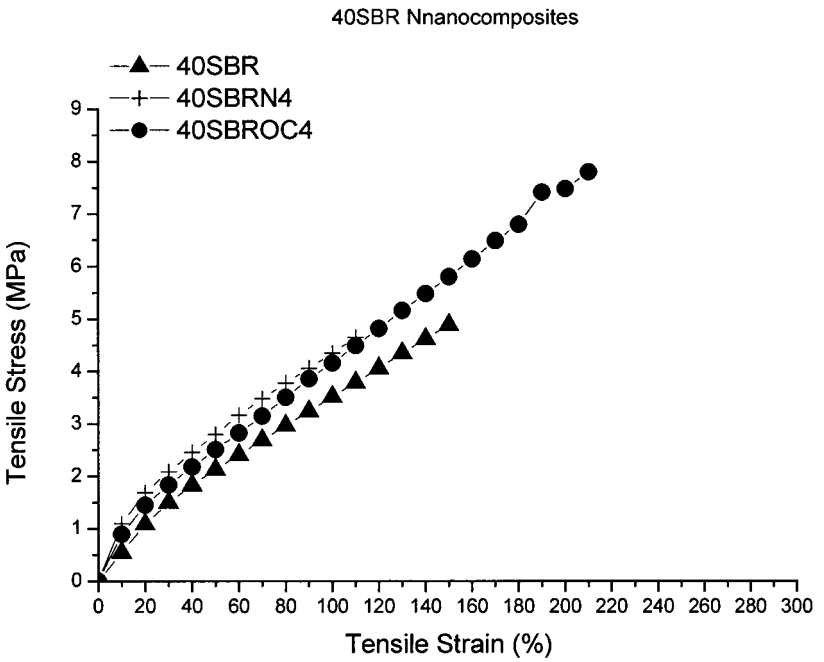

Figure 9 Stress–strain plots of 40SBR with and without clay.

tetrachloride) with different solubility parameters ($\delta_{toluene}$ = 18.2 $cal^{1/2}$ $cm^{-3/2}$, $\delta_{chloroform}$ = 19.0 $cal^{1/2}$ $cm^{-3/2}$, and $\delta_{carbon\ tetrachloride}$ = 17.6 $cal^{1/2}$ $cm^{-3/2}$) were chosen. The mechanical properties, given in Table V, indicated that 23SBROC4s prepared in the three different solvents were not identical. The tensile strength of 23SBROC4 was 2.5 MPa, whereas the values for Ca-23SBROC4 and Ch-23SBROC4 were 2.43 and 2.2 MPa, respectively. The elongations at break were 167, 277, and 525% for 23SBROC4, Ca-23SBROC4, and Ch-23SBROC4, respectively. Similarly, the values of the modulus at 50% elongation were 0.77, 0.54, and 0.44 MPa. These values were averages of repeat measurements and were distinctly different, even with consideration given to the maximum errors of the measurements. The highest tensile strength was for a toluene-cast sample, whereas the highest elongation at break was observed when the

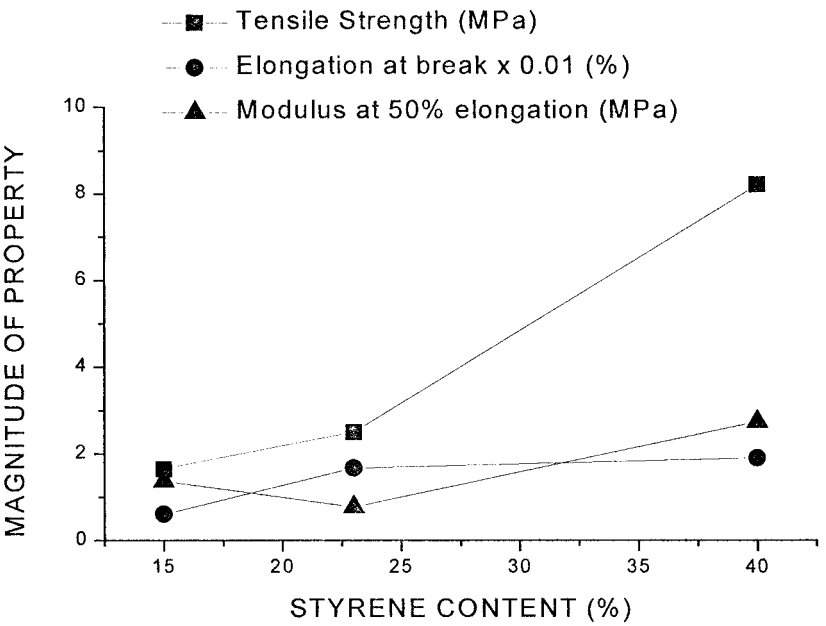

Figure 10 Variation of the mechanical properties with the styrene content of SBR for SBROC4s.

TABLE V
Results of the Mechanical Properties of the Samples Cast in Various Solvents

Sample	Tensile strength (MPa)	Elongation at break (%)	Modulus at 50% elongation (MPa)	Work to break (J/m^2)
23SBROC4	2.50	167	0.77	911
Ca-23SBROC4	2.43	277	0.56	1587
Ch-23SBROC4	2.20	525	0.44	2727

solvent was chloroform. The XRD results [Fig. 3(c)] showed that there were small humps around 7° for Ca-23SBROC4 and Ch-23SBROC4. However, there was no peak for 23SBROC4. This implied that the clay was fully exfoliated in case of 23SBROC4, probably because of the decoiling of the SBR chains in toluene as a result of similar polarity and solubility parameters. This was probably the reason behind the slightly higher values of the tensile strength and modulus of 23SBROC4 samples, in comparison with the others. Consequently, the elongation at break was higher for Ca-23SBROC4 and Ch-23SBROC4. It was inferred that the nature of the solvent affected the properties of the nanocomposites.

Effect of the curing agents on the mechanical properties of the nanocomposites

Rubbers are cured by various curing agents in actual applications. Therefore, the effects of different curing agents on SBR-based nanocomposite were studied, and the results are listed in Table VI. Two different cure packages (a DCP cure system and a sulfur vulcanization system) were chosen. The dosage of the curing system was optimized in such a way that the values of the volume fraction of rubber (V_r; which is directly proportional to the crosslink density) of both systems were comparable (V_r = 0.119). For the neat rubber vulcanizates, the tensile strength was 2.40 and 2.43 MPa, whereas the elongation at break was 257 and 770% and the modulus was 0.57 and 0.54 MPa for the DCP and sulfur cure systems, respectively. For the unmodified and modified clay–rubber nanocomposites, the trend for the mechanical properties was almost the same as that of the neat vulcanizates. In the case of sulfur curing, there was the formation of polysulfidic bonds, which were flexible and responsible for higher elongation. However, the modulus and tensile strength of both cure systems were almost comparable because of the similar crosslink densities. The difference in the properties of the unmodified and modified clay–rubber systems arose for the reasons given earlier.

TABLE VI
Variation of the Mechanical Properties with the Cure System

Sample	Tensile strength (MPa)	Elongation at break (%)	Modulus at 50% elongation (MPa)	Work to break (J/m^2)
SBR (0.5)	2.40	257	0.57	1476
SBRN4 (0.5)	2.37	247	0.59	1381
SBROC4 (0.5)	2.60	290	0.60	1742
SBR (S)	2.43	770	0.54	4529
SBRN4 (S)	2.40	779	0.51	4429
SBROC4 (S)	2.63	690	0.57	3574

Effect of the variation of the cure time on the nanocomposite properties

The SBR, SBRN4, and SBROC4 samples were cured for four different cure times (10, 15, 30, and 60 min) at 160°C. The mechanical properties are reported in Table VII. The optimum cure time was calculated to be 15 min at 160°C with a standard rheometer. The highest values of the tensile strength (1.20 MPa) and elongation at break (111%) for 23SBR were observed after 15 min of curing. After that, the tensile strength decreased by 25% and the elongation at break decreased by 42% when the samples were cured for 60 min. The modulus increased (9%) with the longer cure. Almost the same trend in the mechanical properties was seen for 23SBRN4. The changes in the tensile strength, elongation at break, and modulus were 9, 20, and 43%,

TABLE VII
Influence of the Cure Time on the Mechanical Properties of the Nanocomposites

Sample	Tensile strength (MPa)	Elongation at break (%)	Modulus at 50% elongation (MPa)	Work to break (J/m^2)
23SBR-10	1.20	101	0.66	296
23SBRN4-10	1.70	155	0.60	547
23SBROC4-10	2.60	177	0.74	1199
23SBR-15	1.20	111	0.66	284
23SBRN4-15	1.80	152	0.58	606
23SBROC4-15	2.50	167	0.77	911
23SBR-30	1.10	81	0.71	148
23SBRN4-30	1.63	118	0.82	473
23SBROC4-30	2.10	167	0.62	1086
23SBR-60	0.90	64	0.72	149
23SBRN4-60	1.63	121	0.83	507
23SBROC4-60	2.10	168	0.66	802

TABLE VIII
Effect of Aging on the Mechanical Properties of the Nanocomposites

Sample	Conditions (h/°C)	Tensile strength (MPa)	Elongation at break (%)	Modulus at 5% elongation (MPa)
23SBR	36/100	1.2	84	0.11
23SBRN4		1.9	46	0.16
23SBROC4		2.2	70	0.18
23SBR	36/120	2.3	12	1.17
23SBRN4		5.2	5	5.20
23SBROC4		6.5	6	6.07
23SBR	72/100	2.3	10	1.70
23SBRN4		5.1	5	5.10
23SBROC4		5.6	7	5.20

respectively, for 23SBRN4 cured for 60 min. 23SBROC4, however, did not display remarkable changes (except for the modulus) with the variation of the cure time.

The results can be explained as follows. All the rubber vulcanizates had an optimum cure time, which depended on the temperature. After the optimum cure time, the minor decrease in the properties was due to the overcuring of SBR, which led to either resin formation or scission. In this case, the increase in the modulus indicated the resin formation of SBR, which was the reason for the decrease in the elongation at break. The interplay of gelling, resin formation, or scission is responsible for the variations in the properties.

Effect of aging on the nanocomposite properties

To understand the effect of aging, we used three different aging conditions (36 h at 100°C, 36 h at 120°C, and 72 h at 100°C). The results are reported in Table VIII. In all cases, the tensile strength increased and the elongation at break decreased significantly with aging. The modulus at 5% (as most of the sample broke within 10% elongation) also increased with the time or temperature of aging. The aging of SBR has been extensively reported in the literature.[18] The scission of the main chain or crosslinks and resin formation took place during aging. The possibility of crosslinks through residual peroxide in the initial stage could not be ruled out. Although the swelling data did not identify the exact reasons, the scission reactions seemed to predominate at aging for 36 h at 100°C, following the earlier references. At higher temperatures or longer times of aging, the strength and modulus improved because of resin formation and gelling. The incorporation of clay deteriorated the aging properties of SBR (16–50% decrease in the elongation at break, depending on the aging conditions in SBROC4 with respect to the control). The modified clay did not improve the oxidative aging properties significantly, although a few aging properties were better in the modified clay system. Thus, the extended aging of the samples led to higher stiffness and higher tensile strength but reduced elongation at break. The results showed that a higher temperature was more effective than a longer aging time in changing the properties in this case. The tensile strength of SBR changed from 2.3 to 6.5 MPa with the aging of SBROC4 for 36 h at 120°C. The change in the elongation at break for the same was 6%.

CONCLUSIONS

1. Montmorillonite clay was modified with octadecyl amine. Upon the incorporation of this modified clay, the tensile strength, elongation at break, and modulus of SBR improved, even with a very low degree of filler loading, because of the exfoliation of the clay, as observed in XRD studies.
2. The effects of the styrene content on the mechanical properties were studied. Increasing the styrene content increased the tensile strength, modulus, and elongation at break of SBR. Upon the incorporation of both clays, the extent of the increase in the properties was much higher for the rubber with a higher styrene content and with modified clay. The improvement in the strength for 40SBR was 53%, whereas the same for 23SBR and 15SBR was 38 and 13%, respectively. The XRD data showed that the clays were totally exfoliated in all the modified clay–rubber composites. The TEM photomicrographs provided a clear indication of the formation of nanocomposites. The FTIR data of the composites did not show any remarkable change due to the addition of the modified clay in the rubber.
3. The solvent used in the nanocomposite preparation influenced some of the properties. There was a significant change in the elongation at break, but the strength values were comparable. The modulus values were lower for samples cast from chloroform and carbon tetrachloride.
4. The cure system had a very prominent effect on the elongation at break of the composites. The strength and modulus were comparable in both the DCP and sulfur cure systems with the same crosslink density. However, the elongation at break was significantly higher for the sulfur cure system.
5. The strength and elongation at break were optimum at the optimum cure time, beyond which there was a drop in the properties. The modulus, however, increased. Upon the modification of the clay, the trend in the properties was the same. However, the strength, elongation at break, and modulus were higher than those of unmodified clay–rubber vulcanizates.

6. The aging studies showed that among the three aging conditions—36 h at 100°C, 36 h at 120°C, and 72 h at 100°C—the effect of aging was most pronounced with the second, and this was reflected in the properties. The elongation at break decreased to a great extent, whereas the modulus and strength increased. Here again, the mechanical properties were better in modified clay nanocomposites than in unmodified clay rubber nanocomposites and gum vulcanizates.

References

1. Kojima, Y.; Usuki, A.; Kawasumi, M.; Fukushima, Y.; Okada, A.; Kurauchi, T.; Kamigaito, O. J Mater Res 1993, 1185, 8.
2. Kojima, Y.; Usuki, A.; Kawasumi, M.; Okada, A.; Kurauchi, T.; Kamigaito, O. J Polym Sci Part A: Polym Chem 1993, 1755, 31.
3. Lepoittevin, B.; Devalckenaere, M.; Pantoustier, N.; Alexandre, M.; Kubies, D.; Calberg, C.; Jerome, R.; Henrist, C.; Cloots, R.; Dubois, P. Polymer 2002, 4017, 43.
4. Usuki, A.; Koiwai, A.; Kojima, Y.; Kawasumi, M.; Okada, A.; Kurauchi, T.; Kamigaito, O. J Appl Polym Sci 1995, 119, 55.
5. Shelley, J. S.; Mather, P. T.; DeVries, K. L. Polymer 2001, 5849, 42.
6. Hambir, S.; Bulakh, N.; Kodgire, P.; Kalgaonkar, R.; Jog, J. P. J Polym Sci Part B: Polym Phys 2001, 446, 39.
7. Ma, J.; Qi, Z.; Hu, Y. J Appl Polym Sci 2001, 3611, 82.
8. Kawasumi, M.; Hasegawa, N.; Kato, M.; Usuki, A.; Okada, A. Macromolecules 1997, 6333, 30.
9. Fu, X.; Qutubuddin, S. Polymer 2001, 807, 42.
10. Vu, Y. T.; Mark, J. E.; Pham, L. H.; Engelhardt, M. J Appl Polym Sci 2001, 1391, 82 and references therein.
11. Alexandre, M.; Beyer, G.; Henrist, C.; Cloots, R.; Rulmont, A.; Jerome, R.; Duboise, P. Macromol Rapid Commun 2001, 643, 22.
12. Pramanik, M.; Srivastava, S. K.; Samantaray, B. K.; Bhowmick, A. K. J Polym Sci Part B: Polym Phys 2002, 000, 40.
13. Ray, S.; Bhowmick, A. K. Rubber Chem Technol 2001, 835, 74.
14. Mousa, A.; Karger-Kocsis, J. Macromol Mater Eng 2001, 260, 286.
15. Yatsuyanage, F.; Suzuki, N.; Ito, M.; Kaidou, H. Polymer 2001, 9523, 42.
16. Sadhu, S.; Bhowmick, A. K. Rubber Chem Technol 2003, 860, 76.
17. ASTM D 3849. Annu Book ASTM Stand 1990, Part 606, 9.01.
18. DeSarkar, M.; Bhowmick, A. K. Rubber Chem Technol 1997, 855, 70.